Stimulated Optical Emission in Fluorescent Solids. II. Spectroscopy and Stimulated Emission in Ruby

T. H. MAIMAN,* R. H. HOSKINS,* I. J. D'HAENENS, C. K. ASAWA, AND V. EVTUHOV
Hughes Research Laboratories, A Division of Hughes Aircraft Company, Malibu, California
(Received January 27, 1961)

Optical absorption cross sections and the fluorescent quantum efficiency in ruby have been determined. This data has been used to correlate calculations with the analysis of the preceding paper. Stimulated emission from ruby under pulsed excitation has been studied in some detail; the observations are found to depend strongly on the perfection of the particular crystal under study. A peak power output of approximately 5 kw, total output energy of near 1 joule, beam collimation of less than 10^{-2} rad, and a spectral width of individual components in the output radiation of about 6×10^{-4} A at 6943 A have been measured. It is suggested that mode instabilities due to temperature shifts and a time-varying magnetic field are contributing to an oscillatory behavior of the output pulse.

INTRODUCTION

THE purpose of this paper is to describe the results of spectroscopic and stimulated emission experiments on Cr^{3+} in Al_2O_3 (ruby), and to apply the analysis of the preceding paper[1] to these results.

The energy-level diagram for ruby (taken from the work of Sugano and Tanabe[2]) is shown in Fig. 1. Fluorescence in this crystal is easily demonstrated by irradiating it with green light to excite the $^4A_2 \rightarrow {}^4F_2$ transition, violet light to excite the $^4A_2 \rightarrow {}^4F_1$ transition, or ultraviolet to excite a high-lying charge transfer band (not shown in the diagram[3]). The emission spectrum consists of a sharp doublet ($^2E \rightarrow {}^4A_2$) in the red whose components at room temperature are at about 6943 A (R_1) and 6929 A (R_2) with respective half-power spectral widths of 4 and 3 A.

ABSORPTION SPECTRA

The absorption spectrum of ruby taken with a Cary spectrophotometer is shown in Fig. 2. The sample was a 1-cm cube cut with the c axis perpendicular to one pair of faces. The chromium concentration, determined by chemical analysis, was 0.0515 ± 0.0005 weight percent of Cr_2O_3: Al_2O_3 corresponding to a chromium ion density $N_0=1.62\times10^{19}/cm^3$. Absorption cross sections were calculated using $\sigma=\alpha/N_0$, where α is the linear absorption coefficient.

The absorption data for the R lines (Fig. 2) is inaccurate because of insufficient resolution; therefore, an independent experiment was performed using a ruby optical-maser source to measure transmission through the cube. It was found that with light propagating parallel to the c axis the absorption coefficient for the R_1 line $\alpha\cong0.4$ cm^{-1} and therefore $\sigma\cong2.5\times10^{-20}$ cm^2.

FLUORESCENT EFFICIENCY

A parameter of particular interest in the study of fluorescent solids is the fluorescent quantum efficiency, defined as the ratio of the number of fluorescent photons emitted to the number of exciting photons *absorbed*. Wieder[4] reported 10^{-2} for this quantity, whereas Maiman[5] obtained a value near unity for excitation into the center of the green band. These measurements were repeated and extended to cover excitation in the spectral range of 3500–6000 A.

The sample used was the ruby cube referred to above

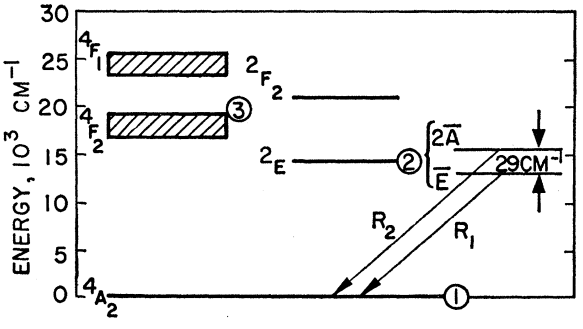

FIG. 1. Energy-level diagram for ruby.

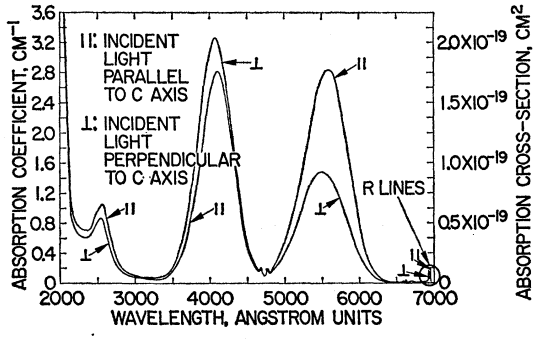

FIG. 2. Spectrophotometric absorption spectrum of ruby. The absorption cross section σ (right scale) is given by $\sigma=\alpha/N_0$, where α is the linear absorption coefficient and N_0 the number of absorbing centers per cm^3.

* Now at Quantatron, Inc., 2520 Colorado Avenue, Santa Monica, California.

[1] T. H. Maimam, preceding paper, Phys. Rev. **123**, 1145 (1961). Hereafter referred to as Part I.

[2] S. Sugano and Y. Tanabe, J. Phys. Soc. (Japan) **13**, 880 (1958).

[3] D. McClure, in *Solid-State Physics*, edited by F. Seitz and D. Turnbull (Academic Press, Inc., New York, 1960), Vol. 9.

[4] I. Wieder, Rev. Sci. Instr. **30**, 995 (1959).

[5] T. H. Maiman, Phys. Rev. Letters **4**, 564 (1960).

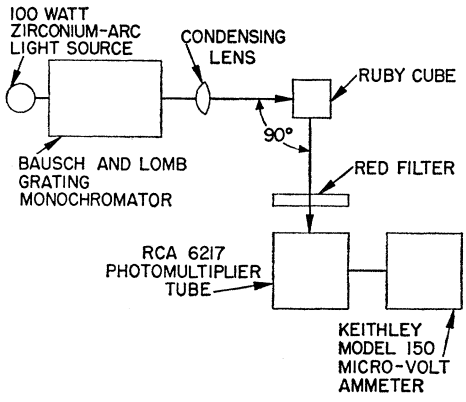

FIG. 3. Block diagram of the experiment setup for the determination of fluorescent efficiency in ruby.

A block diagram of the experiment is shown in Fig. 3. Radiation from a Bausch & Lomb monochromator at a power level of about 25 μw/cm^2 and of 60 A spectral width was incident on a side of the cube normal to the c axis. The total R-line fluorescence radiation was measured both along and normal to the c axis with a photomultiplier tube placed 30 cm from the sample. This light was monitored through a red-transmitting filter and a 0.08-cm^2 aperture. The total radiated power was computed assuming the radiation pattern to be an ellipsoid with an axis of revolution along the crystal c axis.

The light source and monochromator combination was calibrated by replacing the ruby sample by an Eppley silver-cadmium thermopile. The photomultiplier was calibrated by replacing the ruby by a mirror and comparing the resultant photomultiplier reading with that of the thermopile in the same position. In making the latter measurement a calibrated neutral-density (2.0) filter was used with the photomultiplier.

The fluorescent quantum and power efficiencies were calculated from these measurements making use of the data of Fig. 2 and accounting for multiple reflections in the crystal. The results are shown in Fig. 4. The accuracy of the dotted portions of the curves is lower than in the solid portion because of low absorptivity, and hence low absorbed power in the crystal in these regions, which reduces the precision of the measurements. The accuracy of the results in the solid portion of the curves is estimated to be within 10%.

The indicated results of about 70±5% can probably be accounted for by the following argument. The fluorescent lifetime of $^2E \rightarrow {}^4A_2$ is 4.3 msec at 77°K[6] but is reduced to 3.0 msec at 300°K.[5] Estimates of the variation of the matrix elements with temperature indicate a much smaller change than this; therefore, we assume that the reduced lifetime at 300°K is due to thermal relaxation and this alone would restrict the fluorescent quantum efficiency to a maximum of 70% at this temperature.

STIMULATED EMISSION

Pumping Power Considerations

We now consider the amount of input power required to produce oscillations. The thermal relaxation time between the excited states $2\bar{A}(^2E)$ and $\bar{E}(^2E)$ at room temperature is estimated to be the order of one μsec or less, whereas the lifetime of ^2E at this temperature is 3.0 msec.[5] For this reason it can be assumed that the components of ^2E are nearly in thermal equilibrium in the experiments to be described. Because of a somewhat greater population in $\bar{E}(^2E)$ with respect to $2\bar{A}(^2E)$, due to the Boltzmann factor and because the matrix element for the transition $\bar{E}(^2E) \rightarrow {}^4A_2$ is larger than that for $2\bar{A}(^2E) \rightarrow {}^4A_2$, the former transition (R_1) will be favored in stimulated emission experiments.

It was shown in Part I that the excess population needed to produce oscillation is

$$(N_2-N_1)/N_0 \cong (1-r)/\alpha_0 l.$$

In the case considered here, N_2-N_1 is the population excess of $\bar{E}(^2E)$ with respect to $^4A_2$. If we use $\alpha_0 \sim 0.4$ cm^{-1}, $l=2$ cm, and $(1-r)=0.015$ (evaporated silver at 6943 A), we find $(N_2-N_1)/N_0 \approx 0.019$. Thus, only a small excess over equal populations is required.

A simple extension of the discussion in Part I indicates that equal populations will be produced when

$$W_{13} \cong (1+e^{-h\nu_a/kT})A_{21}, \quad (1)$$

where ν_a is the frequency of the transition

$$2A(^2E) \rightarrow E(^2E).$$

This implies an energy density of pump radiation

$$U_p = (1+e^{-h\nu_a/kT})A_{21}h(\sqrt{\epsilon})/\lambda_p \sigma_p. \quad (2)$$

If the crystal is illuminated uniformly with isotropic

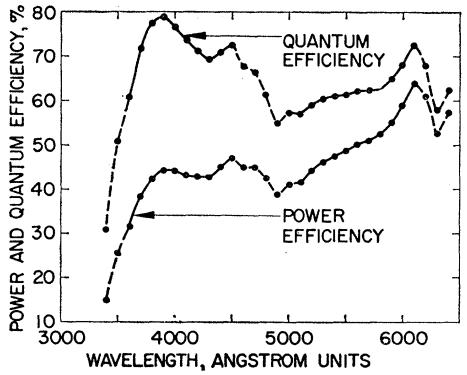

FIG. 4. Fluorescent quantum and power efficiencies for ruby: ratio of output fluorescence to input absorption as a function of wavelength.

[6] F. Varsanyi, D. A. Wood, and A. L. Schawlow, Phys. Rev. Letters 3, 544 (1959).

radiation,

$$F=\frac{c}{4\sqrt{\epsilon}}U_p=\frac{(1+e^{-h\nu_a/kT})h\nu_p A_{21}}{4\sigma_p}. \quad (3)$$

Substituting the values applicable to ruby, i.e.,

$$\sigma_p=10^{-19}\ \text{cm}^2,\quad \nu_a=8.7\times10^{11}/\text{sec},\quad \nu_p=5.4\times10^{14}/\text{sec},$$
$$A_{31}=330/\text{sec};$$

we find that $F>555$ w/cm^2 is required to produce stimulated emission in this crystal.

Because of the broad spectral distribution of typical high-intensity exciting sources,[1] it is interesting to consider the brightness and spectral efficiency of a blackbody radiator in this connection. The flux density and relative spectral efficiency of such a radiator are given in Figs. 5 and 6. Radiation centered at both 5500 and 4100 A and 1000 A wide are considered, corresponding approximately to the green and violet bands in ruby. If we consider excitation into the green band only, for the moment, it is seen that a radiation temperature of about 5250°K is required for the onset of stimulated emission and that reasonable spectral efficiencies would be realized up to perhaps 15 000°K. Excitation into the violet band is not as efficient from a power standpoint (see Fig. 4) as the green band. Also, a side effect is possible from violet radiation. Maiman[5] has shown that appropriate wavelengths can stimulate transitions from ^2E to the charge transfer band; therefore, at high power densities, where the population of ^2E is appreciable, the net effect of the blue radiation could easily be to *de*populate ^2E.

Due to the need for high source intensities to produce stimulated emission in ruby and because of associated heat dissipation problems, these experiments were performed using a pulsed light source. For the case in which the exciting light pulses are short compared to the fluorescent lifetime, the requirement on the flash tube

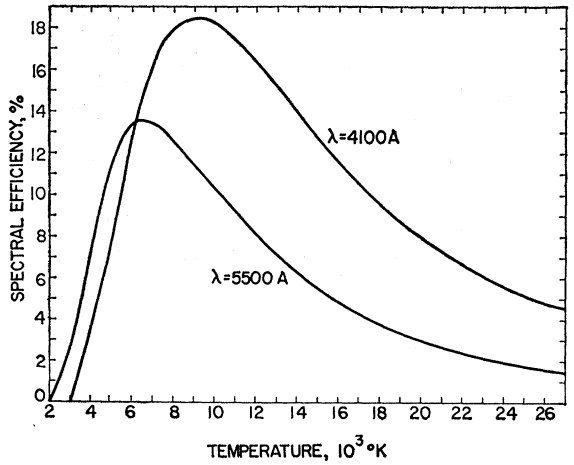

FIG. 5. Fraction of radiation from a blackbody in 1000 A interval centered at 5500 A and 4100 A as a function of temperature.

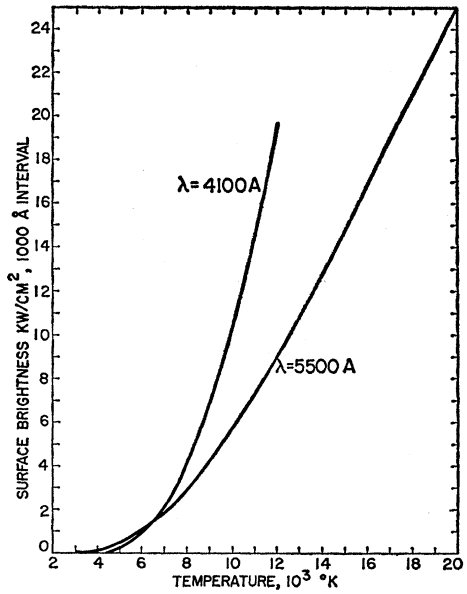

FIG. 6. Surface brightness from a blackbody in 1000 A interval centered at 5500 A and 4100 A as a function of temperature.

is that the energy per unit area[1] is

$$J=(1+e^{-h\nu_a/kT})h\nu_p/4\sigma_p; \quad (4)$$

for ruby, this requirement is $J\cong1.67$ joules/cm^2.

The source which was used was a General Electric type FT-506 xenon-filled quartz flash tube; this tube has a luminous efficiency of 40 lumens per watt. By coincidence, the green absorption band of ruby is almost identical to the sensitivity response of the human eye; therefore, lumens are meaningful units in this experiment corresponding to 0.0016 w of radiant energy and the spectral efficiency of the lamp is therefore about 0.064. The radiating area of this source is approximately 25 cm^2 so that an electrical input energy to the lamp of 650 joules would be required to produce stimulated emission in ruby on the basis of the previous considerations.

Apparatus

The material samples were ruby cylinders about $\frac{3}{8}$ in. in diameter and $\frac{3}{4}$ in. long with the ends flat and parallel to within $\lambda/3$ at 6943 A. The rubies were supported inside the helix of the flash tube, which in turn was enclosed in a polished aluminum cylinder (see Fig. 7); provision was made for forced air cooling. The ruby cylinders were coated with evaporated silver at each end; one end was opaque and the other was either semitransparent or opaque with a small hole in the center.

A block diagram of the experiment is shown in Fig. 8. The energy to the flashtube was obtained by discharging a 1350-μf capacitor bank and the input energy was varied by changing the charging potential. The R_1 output radiation was monitored with a type 6217 photo-

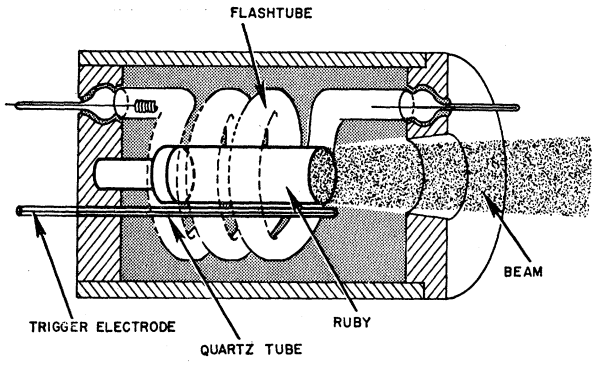

FIG. 7. Apparatus for pulsed excitation of ruby. (Actual size, approximately 2×1 in. o.d.)

multiplier tube which was calibrated at 6943 A by comparison with an Eppley thermopile to radiation at this wavelength in a band 200 A wide. The thermopile was calibrated with an NBS standard lamp. The attentuation of the radiation necessary to insure linear response of the photomultiplier was obtained by the use of calibrated neutral-density gelatin filters. Peak output power and details of the output pulse were obtained from the phototube output across a 1000-ohm resistor on an oscilloscope; the total instrumental response time was about 0.1 μsec. The total energy in the output pulse was obtained by integrating the phototube current with a 0.1-μf mica capacitor.

Experimental Results

1. Summary

It was found with high-intensity excitation that the nature of the output radiation from the various ruby samples which were tried could be divided into two categories:

A. Crystals which exhibited R_1 line narrowing of only 4 or 5 times, a faster but smooth time decay of the output (compared to the fluorescence), an output beam angle of about 1 rad, and no clear-cut evidence of a threshold excitation. This type of behavior was reported and discussed by Maiman.[7]

B. Crystals which exhibited a pronounced line narrowing of nearly four orders of magnitude, an oscillatory behavior of the output pulse, and a beam angle of about 10^{-2} rad; these crystals were particularly characterized by a very clear-cut threshold input energy where the pronounced line and beam narrowing occurred. This second category of behavior was reported by Collins *et al.*,[8] and is the subject of further study reported here.

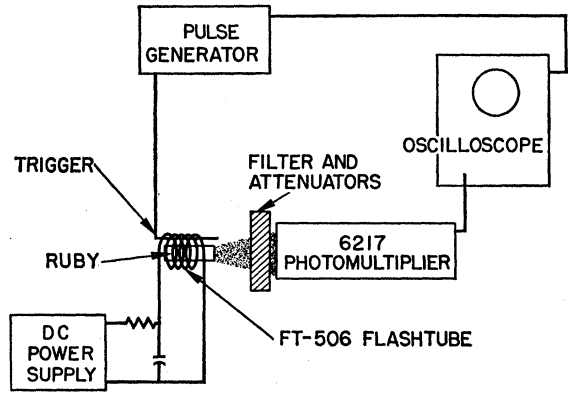

FIG. 8. Block diagram of experimental setup for the observation of stimulated emission in ruby.

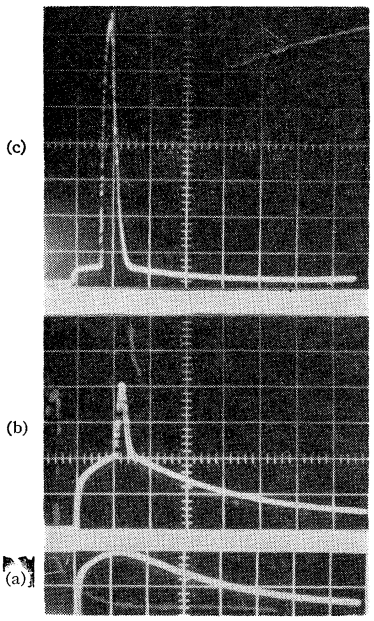

FIG. 9. R_1 line output pulse with various input energies: (a) below threshold, (b) threshold, (c) above threshold. The instrumental response time is too long to resolve the oscillatory structure of the stimulated emission pulse.

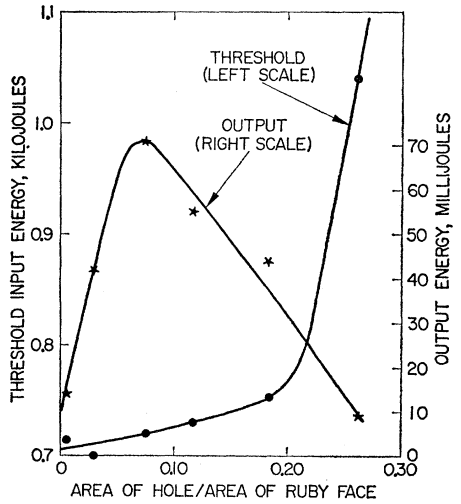

FIG. 10. Input electrical energy for the threshold of stimulated emission and stimulated emission output energy with an input of approximately twice threshold as a function of degree of coupling to the ruby. Coupling was changed by varying the size of a hole in one totally reflecting end.

[7] T. H. Maiman, British Communications and Electronics **7**, 674 (1960); Nature **187**, 493 (1960).

[8] R. J. Collins, D. F. Nelson, A. L. Schawlow, W. Bond, C. G. B. Garrett, and W. Kaiser, Phys. Rev. Letters **5**, 303 (1960).

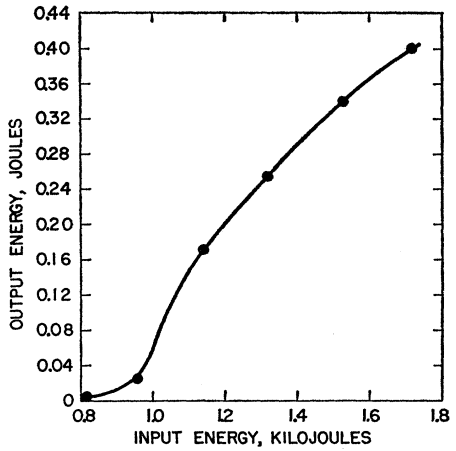

FIG. 11. Stimulated emission output energy from a ruby with a semitransparent (7% transmitting) end face as a function of electrical energy input to the exciting lamp source.

2. *Threshold*

The R_1 output light at various levels of input illumination is shown in Fig. 9. The spontaneous fluorescent radiation is shown in (a). In (b), the input energy has been increased by approximately one part in 10^4 and the onset of stimulated emission can clearly be seen. We define this condition as threshold. In (c) (different vertical scale), the input energy has been increased still further and the stimulated emission is seen to increase rapidly over the spontaneous fluorescent radiation. The instrumental response time for these particular photographs was long; hence, the structure of the stimulated emission pulse (discussed below) is not seen.

The variation in input energy required for the onset of stimulated emission as a function of degree of coupling to the ruby is shown in Fig. 10. Coupling was varied by gradually enlarging a small hole in the center of one of the silvered ends of the ruby. The abscissa of the curve is the ratio of the area of the unsilvered hole to the total area of the face. Variation in coupling was also obtained by changing the thickness of a partially transmitting silver film on one end of the ruby. The latter mathod is more suitable to analytic treatment of the data; however, in practice, it is much more difficult to take the ruby from its holder, remove a silver film, and resilver in a controlled manner than simply to enlarge a hole without changing any other experimental conditions.

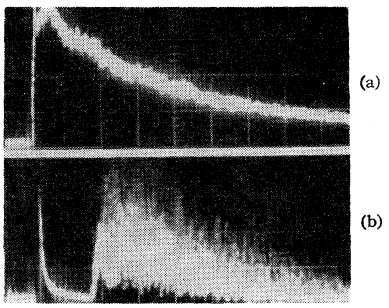

FIG. 12. Light output pulse from the exciting lamp in the green (a) and stimulated emission output pulse from ruby (b) (time scale 200 μsec/division). The excitation energy for (b) was approximately twice threshold. The initial spike in (b) is an electrical transient arising from the trigger circuitry.

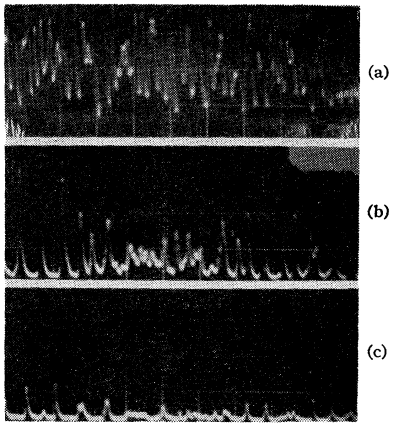

FIG. 13. Output pulse from ruby on an expanded time scale (10 μsec/division). (a), (b), and (c) represent the output approximately 600, 1000, and 1200 μsec after the onset of oscillation. The vertical sensitivity and the base line are the same in each case.

The qualitative behavior shown in the figure is expected, since increasing the hole size reduces the effective reflection coefficient of the end face; a larger population excess is then required, which in turn requires larger input energy to the system. When the hole size becomes sufficiently large, the necessary excess population to overcome the cavity losses is not attainable at any value of pumping energy.

3. *Output Energy and Peak Power*

The variation of the total energy output with size of coupling hole at a fixed energy input (approximately twice threshold energy for small coupling) is also shown in Fig. 10. An optimum hole size for maximum energy output (which varies with available input energy and from sample to sample) is clearly indicated. This vari-

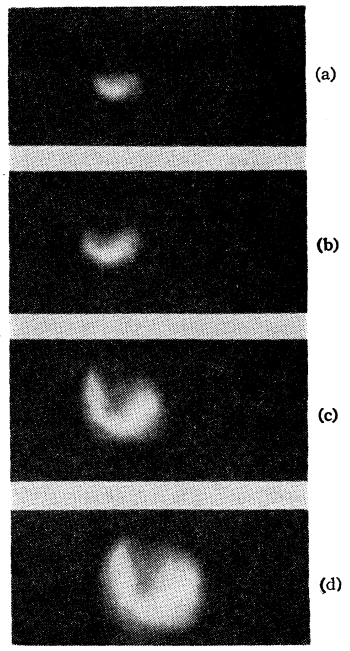

FIG. 14. Change in stimulated emission output beam with input energy for a ruby with a small hole in one totally reflecting end. The angular width of the largest pattern is about 1°.

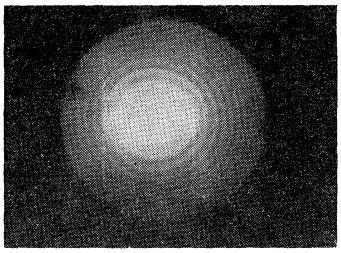

FIG. 15. Output beam pattern for a partially silvered ruby.

ation is also readily understood in terms of coupling to a resonant cavity. The peak power output follows a similar curve.

The energy output from a ruby with a partially silvered end face (7% transmitting) as a function of electrical energy input to the flash tube is given in Fig. 11. The slow initial rise of the curve is due to integration of spontaneous fluorescent radiation which makes up a relatively large portion of the light reaching the phototube detector at input energy levels near threshold. At higher input energies, the curve rises more rapidly as the spontaneous emission radiation becomes smaller in relation to the total output. Since the efficiency of the flash tube increases as the input energy increases, the curve does not represent light output as a function of *light* input. The peak power output, difficult to determine closely because of the pulsed nature of the radiation, again follows the same general curve, but with a faster initial rise, since the spontaneous emission is not integrated. Under the conditions of Fig. 11, the peak output power with 1730 joule input was more than 3 kw and the total output energy was 0.4 joule (using a different ruby sample, a peak power output in excess of 5 kw and an integrated output energy of near 1 joule was measured).

Characteristics of Emitted Radiation

The exciting flash tube output in the green and the stimulated emission pulse with an input approximately twice threshold are shown in Fig. 12, the time scale for both traces being 200 μsec/division. The stimulated emission pulse (b) is seen to lag the input pulse (a) by approximately 300 μsec, the time required for the buildup of excess population in the ^2E level. The output pulse from a ruby with a 3% transmitting silver film on one end with an excitation energy approximately twice threshold is shown in Fig. 13 on an expanded time scale. The amplitude of the individual pulses making up the output are seen to vary in an erratic manner and the average pulse repetition rate is seen to decrease markedly as the input light intensity decays. The rise time of the pulses approaches the instrumental rise time of $\sim$0.1 μsec and does not appear to depend upon the excitation level. No apparent variation of pulse repetition rate or rise time as a function of coupling was found.

Mode selection by means of the following experiment was tried. The silver coating from one end of the crystal was removed and replaced by a mirror parallel to and 5 cm from this end of the ruby. The beam angle decreased and the oscillatory behavior of the output changed, exhibiting a much greater separation between the individual pulses.

The spatial nature of the stimulated emission from a ruby with a small coupling hole varies in an interesting way from that from the same ruby with a partially transmitting end coating. For a particular ruby with a 0.125-in. coupling hole in a totally reflecting end coating, the nature of the spot varied with input power as shown in Fig. 14. The image of the spot on a transluscent screen located 75 cm from the end of the ruby was photographed from behind the screen. At input energies just above threshold, the output starts as a barely discernible, small, approximately round spot not shown in the figure. As the input energy increases, the spot spreads in two directions to form, at input levels approximately twice threshold, a horseshoe shaped pattern of approximately one degree angular width.

The same ruby with a partially transmitting end coating gives, slightly above threshold, a small round spot (of smaller linear dimension than the ruby face at close distances) surrounded by barely discernible rings. As the input energy is increased, the central spot appears to grow and fill in the space between the rings. Such behavior might arise if only a portion of the ruby were active. As the input energy is increased, the active portion of the ruby increases in size. The ring pattern from another ruby with a partially transmitting end is shown in Fig. 15. The size of the central spot projects to about 3 mm in diameter at the face of the ruby (the diameter of the ruby is about 9 mm) and has an angular width of 10^{-2} rad. The angular diameter of the rings varies as $(n+a)^{\frac{1}{2}}$, where n is an integer and a is a constant. The appearance of these rings is discussed by Wagner and Birnbaum[9] and explained on the basis of a Fabry-Perot type phenomena within the ruby.

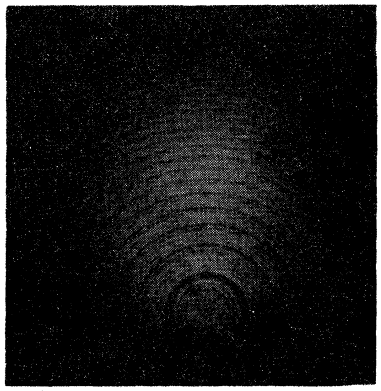

FIG. 16. Stimulated emission from ruby as observed through a Fabry-Perot interferometer having an 18.5-cm plate separation (interorder spacing 0.0135 A). Bright fringes are the white areas of the figure.

[9] W. G. Wagner and G. Birnbaum (to be published).

The spectral width of the emitted radiation was investigated with a Fabry-Perot interferometer. In general, one or more sharp components were observed of spectral width $\sim 6\times 10^{-4}$ A superimposed on a broader background (see Fig. 16). The fringe patterns were not, however, reproducible; that is, the number and relative intensity of the components changed in each photographic exposure.

DISCUSSION

The variation in the behavior of stimulated emission in ruby can be explained on the basis of the discussion in Part I. It was asserted that badly strained crystals scatter the energy into many cavity modes and that from the curves presented there it was expected that a clearly defined threshold would not be present in such cases. This is corroborated by the fact that the rubies which exhibit the pronounced beam and spectral narrowing, when viewed with polarized light, appear to be less strained than the others.

Several theories to account for the oscillatory nature of the output based upon relaxation behavior have been advanced.[8,10] There is, however, a possibility that some type of mode-hopping process is also taking place, since the frequency of the inverted transition is certainly being swept in time during the oscillation pulse due to temperature changes and also due to a time-varying magnetic field produced by the current flow in the helical flash tube. Moreover, it is difficult to explain the appearance of several extremely narrowed lines observed with the Fabry-Perot interferometer unless some sort of mode sweeping is invoked. Further experimental work is indicated before the characteristics of the emitted light can be fully understood.

ACKNOWLEDGMENTS

The authors are indebted to R. C. Pastor and H. Kimura for the chemical analysis of the rubies, to J. Bernath and M. Himber for the frabrication of the ruby samples, and to C. R. Duncan for the electronic instrumentation. We have benefited from helpful discussions with G. Birnbaum, R. W. Hellwarth, and W. G. Wagner.

[10] R. W. Hellwarth, Phys. Rev. Letters 6, 9 (1961).

PHYSICAL REVIEW VOLUME 123, NUMBER 4 AUGUST 15, 1961

Lattice Dynamics of Alpha Uranium*

D. O. Van Ostenburg
Argonne National Laboratory, Argonne, Illinois

(Received September 14, 1960; revised manuscript received December 27, 1960)

The method developed by Begbie and Born has been applied to alpha uranium, where equations are developed which give the macroscopic elastic constants in terms of the microscopic force constants. Interactions of an atom with its first through fourth nearest neighbors, which involve twelve atoms, are considered. Through symmetry considerations, nineteen atomic force constants enter into this force system. An independent determination of the force constants is required before a valid verification of the solutions can be made. However, using measured values of the nine elastic constants, two sets of force constants are evaluated, one based upon quasi-central forces and the other upon neglect of fourth nearest neighbors.

I. INTRODUCTION

BEGBIE and Born[1] developed the so-called "method of long waves" in order to study the relationship between elastic constants and atomic force constants. In their development the atomistic equations of motion are expressed in terms of the second derivatives of the potential energy function with respect to atomic displacements. These derivatives termed the atomic force constants are general in the sense that no assumption is made regarding the form of the potential. The elastic constants are obtained in terms of these atomic force constants by comparing these atomistic equations of motion with the elastic equations for a macroscopic medium.

The structure of alpha uranium can be described as a close-packed hexagonal lattice that has been distorted to orthorhombic symmetry. Choosing any particular atom as origin, it has two nearest, two second nearest, four third nearest, and four fourth nearest neighbors. The structure may be viewed as two interpenetrating side-centered orthorhombic lattices with a unit cell containing two atoms. Using symmetry considerations it is possible to study the interactions of an atom with its first through fourth nearest neighbors in terms of nineteen atomic force constants.

In what follows, we develop equations which express the nine elastic constants in terms of these nineteen

* This work was carried out under the auspices of the U. S. Atomic Energy Commission.

[1] G. H. Begbie and M. Born, Proc. Roy. Soc. (London) **A188**, 179 (1947); G. H. Begbie, Proc. Roy. Soc. (London) **A188**, 189 (1947).

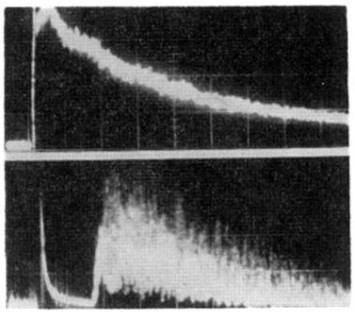

FIG. 12. Light output pulse from the exciting lamp in the green (a) and stimulated emission output pulse from ruby (b) (time scale 200 μsec/division). The excitation energy for (b) was approximately twice threshold. The initial spike in (b) is an electrical transient arising from the trigger circuitry.

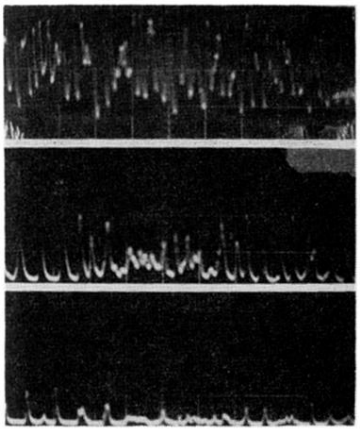

FIG. 13. Output pulse from ruby on an expanded time scale (10 μsec/division). (a), (b), and (c) represent the output approximately 600, 1000, and 1200 μsec after the onset of oscillation. The vertical sensitivity and the base line are the same in each case.

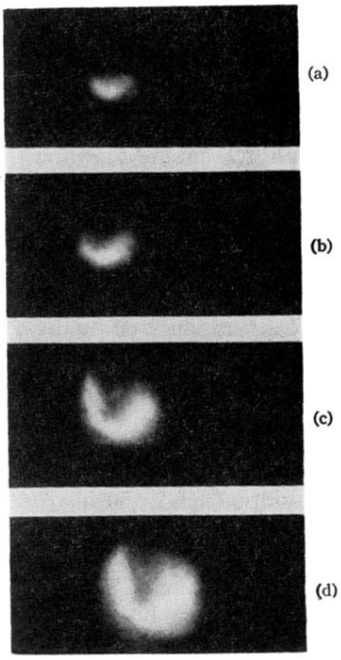

FIG. 14. Change in stimulated emission output beam with input energy for a ruby with a small hole in one totally reflecting end. The angular width of the largest pattern is about 1°.

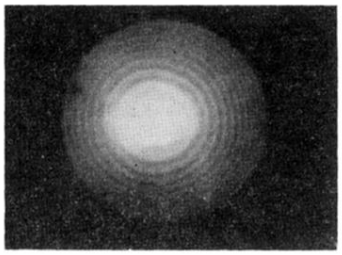

FIG. 15. Output beam pattern for a partially silvered ruby.

FIG. 16. Stimulated emission from ruby as observed through a Fabry-Perot interferometer having an 18.5-cm plate separation (interorder spacing 0.0135 A). Bright fringes are the white areas of the figure.

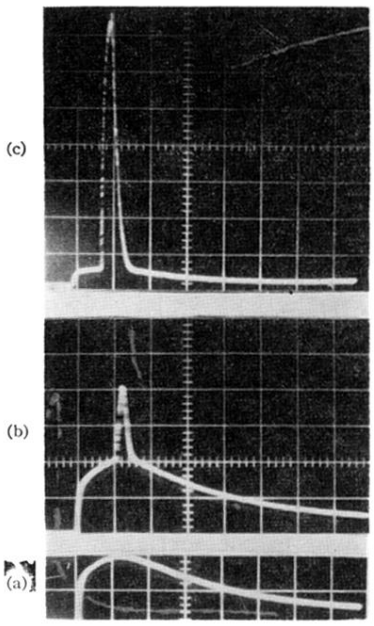

FIG. 9. R_1 line output pulse with various input energies: (a) below threshold, (b) threshold, (c) above threshold. The instrumental response time is too long to resolve the oscillatory structure of the stimulated emission pulse.